Maximum Likelihood Estimation of Synchronous Machine Parameters from Flux Decay Data

A. Tumageanian A. Keyhani S.I. Moon T. Leksan† L. Xu
The Ohio State University
Columbus, OH 43210 U.S.A.

Abstract–A time-domain system identification procedure to estimate the parameters of a 5 kVA salient pole synchronous machine from standstill test measurements is proposed. The test consists of a dc flux decay signal applied to the d-axis and q-axis of the machine. From the recorded responses to this signal, the admittance transfer function models and the SSFR equivalent circuit models are identified. The Maximum Likelihood algorithm is used to estimate the model parameter values, and the Akaike Criterion is used to select the best-fit model. The performance of the standstill models in the dynamic environment is studied through simulation of an on-line small-disturbance test. The results are compared with measured data.

I. Introduction

Standstill frequency response data and time domain response data are used for synchronous machine modeling and parameter estimation [1-9]. The results of the Standstill Frequency Response (SSFR) technique show that the estimated models are sufficiently accurate in the $0.1 - 10$ Hz frequency range [7,8]. Time domain methods have attracted attention due to the relatively simple testing procedures involved. However, these methods have not yet been completely validated against measurements [4,6].

In this paper the machine is identified directly from time-domain standstill test data. A flux decay signal is applied to the d- and q-axis of the machine. The parameters of the admittance transfer function models and the SSFR equivalent circuit models are estimated from this data. The best-fit model from each model set is then selected based on the Akaike Criterion. Lastly, the estimated model performance is evaluated using standstill and small-disturbance measured data.

II. Standstill Flux Decay Testing

The standstill test configuration is shown in Fig. 1. The setup is similar to that described in [6]. A three-phase salient-pole laboratory machine rated 5 kVA and 240 V is tested. A 12 V car battery is used as the input voltage source. The rheostat is used to adjust the input voltage until current less than the machine rating flows in the stator. When switch S_1 is closed, current is supplied to the machine and when S_2 is closed, the flux decay response is initiated. Simultaneously, the data acquisition system is triggered. The current sensors (CS1 and CS2) and voltage sensor (VS) record $v_s(t)$, $i_s(t)$, and $i^*_{fd}(t)$. * denotes the value on the field side, as measured with the machine in the d-axis position. Maximum coupling between the stator and field windings occurs in this position. Minimum coupling exists in the q-axis position. Using Park's transformation, the $d-q$ axis data are obtained from the measured stator quantities (Fig. 1). For estimation purposes, a 0.8 second input-output history is recorded.

The concern in adjusting the dc armature current as described above is to avoid saturating the machine at standstill, and generally, current levels below the rating will achieve this goal. If linear operation of the machine is assumed, then ideally the armature current could be adjusted to any value below the rating. However, for small machines, the lower limit of measurable current is dictated by the sensitivity of the metering equipment used. For large machines, the dc current that can be supplied is limited by the size of the available dc source. For example in [2], the experimenters were able to use currents of approximately 125 A and 190 A for the 1100 MW and 600 MW machines, respectively.

III. Synchronous Machine Models

The synchronous machine can be represented by the Standard, SSFR2, and SSFR3 models. The

†Mr.Leksan is now with Power Technologies, Inc.

0-7803-0634-1/92$03.00 ©IEEE

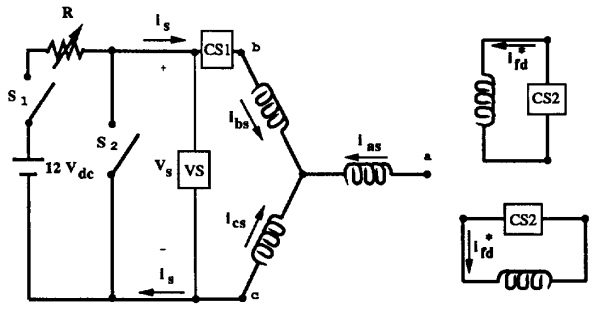

$$V_d = \frac{-V_s}{\sqrt{3}}, \quad i_d = \frac{-2i_s}{\sqrt{3}}, \quad V_q = \frac{V_s}{\sqrt{3}}, \quad i_q = \frac{2i_s}{\sqrt{3}}$$

Fig. 1: Connection diagram for the $d-q$ axis dc flux decay test.

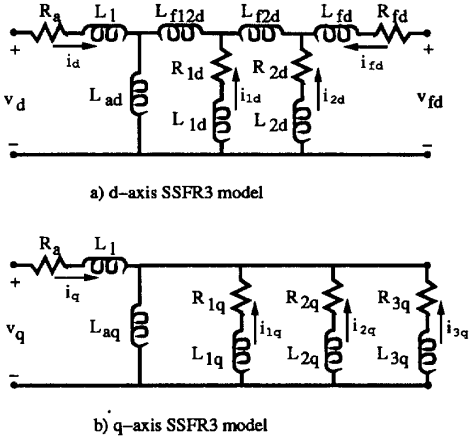

Fig. 2: SSFR3 $d-q$ axis circuit models.

SSFR3 model is shown in Fig. 2. The Standard, SSFR2 and SSFR3 differ in the number of damper windings and leakage inductances that they incorporate.

These models are based on the reciprocal per unit system in which all parameters are referred to the stator. In this study, the field winding current is measured on the field side and is referred to the stator using the equivalent turns ratio, a, between the field and stator:

$$i_{fd} = \frac{2}{3} \cdot a \cdot i^*_{fd}. \tag{1}$$

The field winding resistance value is also referred to the stator side as

$$R_{fd} = \frac{3}{2}\left(\frac{R^*_{fd}}{a^2}\right). \tag{2}$$

The discrete-time representation of the d-axis model of Fig. 2 is written as

$$X(k+1) = A_d \cdot X(k) + B_d \cdot U(k) + w(k) \tag{3}$$

$$Y(k+1) = C_d \cdot X(k+1) + v(k+1) \tag{4}$$

$$U = [v_d] \quad Y = [i_d \; i^*_{fd}]^T \quad X = [i_d \; i^*_{fd} \; i_{1d} \; i_{2d}]^T \tag{5}$$

$w(\cdot)$ and $v(\cdot)$ denote the process and measurement noise, respectively, and T denotes the transpose of the vector. The SSFR3 model parameter vector is

$$\theta_d = [R_a \; R^*_{fd} \; R_{1d} \; R_{2d} \; L_l \; L_{ad} \; L_{fd} \; L_{1d} \; L_{2d} \; L_{f12d} \; L_{f2d} \; a] \tag{6}$$

in which L_{fd} is a stator referred value and the equivalent turns ratio, a, is a parameter to be estimated. The q-axis model of Fig. 2 is similarly modeled.

The computations of the A and B matrices from the continuous time-domain representation are described in [10]. The explicit parameterization of continuous system representation is given in [1].

In this study, voltage is the input signal and current is the output signal. Therefore, the transfer functions are in the form of admittances. With the field winding short-circuited, these transfer functions can be given as

$$\left.\frac{i_d(s)}{v_d(s)}\right|_{v^*_{fd}=0} = \frac{1}{R_a + sL_d(s)} \tag{7}$$

$$\frac{i_q(s)}{v_q(s)} = \frac{1}{R_a + sL_q(s)}. \tag{8}$$

The order of the transfer function is determined by the number of poles in the above equations. The third order d-axis transfer function model can be expressed as

$$\left.\frac{i_d(s)}{v_d(s)}\right|_{v^*_{fd}=0} = \frac{1}{R_a + s(L_\ell + L_{ad})\frac{(1+T'_d s)(1+T''_d s)}{(1+T'_{do} s)(1+T''_{do} s)}} \tag{9}$$

$$= \frac{K(1+T'_{do}s)(1+T''_{do}s)}{(1+T_{d1}s)(1+T_{d2}s)(1+T_{d3}s)}. \quad (10)$$

The relationships between the coefficients of (9) and (10) is quite involved. However, if it is assumed that R_a is very small, then T_{d1} will be the longest time constant and it is related to R_a and L_d. Furthermore, the values of T_{d2} and T_{d3} will approach T'_d and T''_d, respectively.

IV. Maximum Likelihood Estimation

The Maximum Likelihood (ML) estimation method is used for synchronous machine model identification. The covariance of the error between the response of the machine models and the measurement data is defined as

$$R(k) = E[e(k) \cdot e(k)^T] \quad (11)$$

$$e(k) = Y(k) - \hat{Y}(k) \quad (12)$$

where $Y(k)$ is the measured output and $\hat{Y}(k)$ is the estimated output using a particular model. The objective of the Maximum Likelihood identification is to estimate the parameter vector θ which maximizes the likelihood function defined as

$$L(\theta) = \prod_{k=1}^{N} [\frac{1}{\sqrt{(2\pi)^m \det(R(k))}} exp\left(-\frac{1}{2}e^T(k)R^{-1}(k)e(k)\right)] \quad (13)$$

where N denotes the number of data points and m is the dimension of Y.

Maximizing $L(\theta)$ is equivalent to minimizing its negative log function, defined as

$$V(\theta) = -logL(\theta). \quad (14)$$

θ is computed iteratively using Newton's approach. In order to carry out the estimation, $V(\theta)$ is computed at each iteration step. Therefore, $\hat{Y}$(k) must be determined at each step. As $X(k)$ is not known exactly, an optimal observer, the Kalman filter, is used to determine $\hat{Y}(k)$ and $R(k)$ [11].

V. The Akaike Information Criterion

As the number of parameters in a model increases, the cost function $V(\theta)$ will decrease or remain constant. However, as the complexity of a model increases, better initial parameters are needed for convergence of the ML algorithm. If an overfitted model is used, that is, one of higher order than the system under test, the ML estimation algorithm will again encounter numerical stability problems.

Therefore, to select the most suitable model, the model which has 1) the lowest cost function $V(\theta)$ and 2) the lowest order or smallest number of parameters is chosen. However, $V(\theta)$ may decrease as the model order or the number of parameters increases. As a result, this method may select an overfitted model. To avoid this problem, the Akaike Information Criterion (AIC) is used [12]. The AIC is defined as

$$AIC(\hat{\theta}) = -2 * log\ L(\hat{\theta}) + 2 * np \quad (15)$$

where $\hat{\theta}$ is the estimated parameter vector and np is the number of parameters. The model with the minimum AIC value is selected as the best model. An objective measure of the most suitable model is thus available.

VI. D-Axis Transfer Function Model Estimation

A parameter initialization technique must be used that will allow convergence of the ML algorithm to a realistic parameter set. To obtain the initial parameter value of the synchronous inductance, the machine open-circuit and short-circuit test data provided by the manufacturer can be used [13]. L_d is determined to be equal to 0.042 H. The initial value of R_a is calculated as 0.418 Ω from the d-axis flux decay steady-state data.

The graphical technique [4,14] is used to estimate the machine time constants. This technique was originally proposed by deMello for machine parameter estimation using the response due to load rejection tests. However, the procedure herein discussed makes use of the standstill flux decay data, and the graphical procedure is applied to this data to determine the time constant values.

Three time constants (T_{d1}, T_{d2}, T_{d3}) are determined from the graphical method, and the third order transfer function is used to model the response.

TABLE I
D-AXIS TRANSFER FUNCTION MODEL PARAMETER ESTIMATION

	3rd Order		4th Order	
	Init.	Est.	Init.	Est.
$R_a(\Omega)$	0.4180	0.4181	0.4181	0.4180
L_d (H)	0.0420	0.0368	0.0368	0.0372
T_d' (sec)	0.0747	0.0706	0.0706	0.0751
T_d'' (sec)	0.0073	0.0118	0.0118	0.0169
T_d''' (sec)	— —	— —	0.0050	0.0003
T_{do}' (sec)	0.3730	0.7321	0.7321	0.7474
T_{do}'' (sec)	0.0370	0.0167	0.0167	0.0240
T_{do}''' (sec)	— —	— —	0.0050	0.0006
$V(\hat{\theta})$		-3214.8		-3223.2
AIC		-6417.5		-6430.3

Thus, the initial values of T_d' and T_d'' are obtained. T_{do}' and T_{do}'' are initialized arbitrarily as five times T_d' and T_d'', respectively. With the initialization complete, the ML method is applied. It is not known, however, if the third order transfer function best represents the measured response. Therefore, the second through fifth order transfer functions are estimated. Results for the third and fourth order models are given in Table I.

To obtain the initial values of the higher order models, the successive initialization technique is used where the estimated parameters of the lower order model are used as initial values for the next higher order model. The remaining parameters are initialized arbitrarily.

The AIC is used to determine the best fit model as the fourth order model, since it has the minimum value of AIC.

VII. D-Axis Equivalent Circuit Model Estimation

The parameters of the equivalent circuit models are also estimated using the flux decay response data. The Standard, SSFR2, and SSFR3 models are considered. The initial parameter values of the Standard model are obtained from the short circuit and open circuit data, from direct measurement, and from equations developed by Krause [15] relating the time constants to the circuit model parameters. In particular, the field, armature and damper winding parameters, are initialized using equations cited in [14], Appendix 6C. L_ℓ is selected as 2% of the estimated value of L_d.

The value of R_a estimated for the third order d-axis transfer function is used as the initial circuit model value. Its value is fixed for the estimation. R_{fd}^* is obtained by directly measuring the resistance of the field winding with a digital multimeter. The ML estimation is performed and the results for the Standard model are given in Table II.

The Standard and SSFR2 models differ by one parameter, the leakage inductance L_{f12d}. Successive initialization and estimation of the SSFR2 parameters shows that this inductance is nearly zero; the SSFR2 model is therefore the same as the Standard model.

The estimated parameters of the Standard model armature and field windings (R_a, R_{fd}^*, L_l, L_{ad}, L_{fd}, a) are used as the initial values of the SSFR3 field and armature winding parameters. R_a and L_{ad} are fixed for the estimation. Since the SSFR3 rotor body circuit is different from that of the Standard model, the initial damper winding parameters must be recalculated using the relation between the SSFR3 circuit parameters and the fourth order time constants [15]. It is found that including L_{f2d} and L_{f12d} in the SSFR3 model leads to numerical problems, and therefore, these parameters are excluded from the estimation. Results are given in Table II.

From Table II it is seen that the Standard model has the lowest value of AIC. The SSFR3 model has a higher AIC value, which indicates that it is overfitted. Thus, the Standard model is selected as the most suitable d-axis equivalent circuit model.

VIII. D-Axis Model Standstill Validation

In order to validate the models against the standstill flux decay response data, the measured and simulated output data are plotted together. It is found that the measured and simulated output data match very well for the time constant and circuit models discussed. For example, Fig. 3 shows the measured and simulated d-axis stator current $i_d(t)$ responses for the fourth order transfer function model.

IX. Q-Axis Transfer Function Model Estimation

The initial value of the armature inductance, L_q is not available. However, L_q is less than L_d for salient

TABLE II
D-AXIS EQUIVALENT CIRCUIT MODEL PARAMETER ESTIMATION

	Standard		SSFR3	
	Init.	Est.	Init.	Est.
$R_a(\Omega)$	(0.4181)[a]	(0.4181)	(0.4181)	(0.4181)
$R^*_{fd}(\Omega)$	52.24	58.37	58.37	58.33
$R_{1d}(\Omega)$	0.4547	0.6512	0.4663	0.6662
$R_{2d}(\Omega)$	— —	— —	9.380	34.99
L_ℓ (H)	0.0007	0.0001	0.0001	0.0001
L_{ad} (H)	0.0362	0.0365	(0.0365)	(0.0365)
L_{fd} (H)	0.0031	0.0040	0.0040	0.0041
L_{1d} (H)	0.0048	0.0064	0.0075	0.0067
L_{2d} (H)	— —	— —	0.0031	0.0050
a	34.12	38.08	38.08	38.04
$V(\hat{\theta})$		-12081.4		-12082.4
AIC		-24146.6		-24144.2

[a]() indicates value is fixed for estimation.

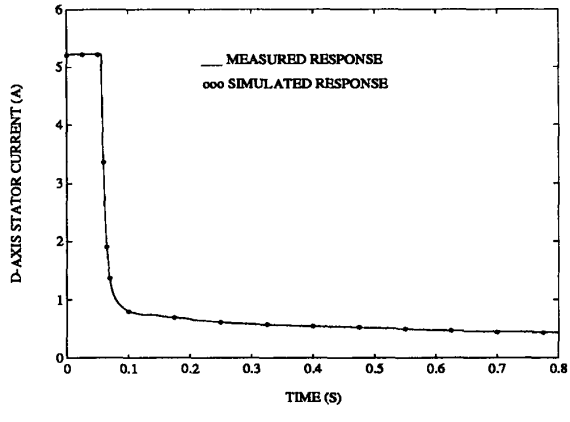

Fig. 3: Measured $i_d(t)$ response and simulated $i_d(t)$ response using the fourth order transfer function model.

pole machines. Therefore, the initial value of L_q is selected as slightly less than the estimated value of L_d of the fourth order model. The initial value of R_a is obtained from the q-axis flux decay steady state data.

To obtain the initial values of the q-axis time constants, the graphical procedure is utilized with the standstill data for the machine in the q-axis position. Three time constants are calculated from the $i_q(t)$ response. With these initial values, the estimation of the third order model is performed.

TABLE III
Q-AXIS TRANSFER FUNCTION MODEL PARAMETER ESTIMATION

	3rd Order		4th Order	
Parameter	Init.	Est.	Init.	Est.
$R_a(\Omega)$	0.4160	0.4162	0.4162	0.4160
L_q (H)	0.0350	0.0243	0.0243	0.0285
T'_q (sec)	0.1690	0.2705	0.2705	1.181
T''_q (sec)	0.0226	0.0164	0.0164	0.0253
T'''_q (sec)	— —	— —	0.0010	0.0069
T'_{qo} (sec)	0.8450	0.3357	0.3357	1.592
T''_{qo} (sec)	0.1130	0.0523	0.0523	0.0669
T'''_{qo} (sec)	— —	— —	0.0050	0.0101
$V(\hat{\theta})$		-3257.0		-3277.9
AIC		-6502.0		-6539.8

The successive initialization scheme is again utilized to initialize the parameters of the higher order transfer function models. The estimation of the transfer function models is performed and the results for the third and fourth order models are shown in Table III. It is found that the AIC values decrease up to the fifth order model, and if the AIC is strictly applied, the fifth order model should be chosen as the best fit model. However, the estimated value of L_q for the fifth order model is larger than the estimated value of L_d. This is not physically realizable. Therefore, the fourth order model is selected as the most suitable q-axis transfer function model.

X. Q-Axis Equivalent Circuit Model Estimation

The $d-q$ axis models share two parameters, R_a and L_ℓ. The estimated d-axis values of R_a and L_ℓ are therefore used for the q-axis estimation. This reduces the number of parameters to be estimated by two. Since the Standard model was chosen as the best fit d-axis circuit model, the values of R_a and L_ℓ of this model are chosen and fixed for the estimation. L_{aq} is calculated by subtracting L_ℓ from L_q, estimated using the third order time constant model.

The initial values of the damper parameters are obtained by the method presented previously: relating the circuit parameters to the time constant

TABLE IV
Q-AXIS EQUIVALENT CIRCUIT MODEL PARAMETER ESTIMATION

	Standard-SSFR2		SSFR3	
	Init.	Est.	Init.	Est.
$R_a(\Omega)$	(0.4181)[a]	(0.4181)	(0.4181)	(0.4181)
$R_{1q}(\Omega)$	0.3676	0.4177	0.0591	0.0401
$R_{2q}(\Omega)$	0.5366	0.5341	0.4313	0.5994
$R_{3q}(\Omega)$	— —	— —	2.114	2.829
L_ℓ (H)	(0.0001)	(0.0001)	(0.0001)	(0.0001)
L_{aq} (H)	0.0241	0.0244	(0.0244)	(0.0244)
L_{1q} (H)	0.0992	0.1170	0.0696	0.1402
L_{2q} (H)	0.0086	0.0087	0.0108	0.0132
L_{3q} (H)	— —	— —	0.0145	0.0168
$V(\hat{\theta})$		-3247.9		-3264.0
AIC		-6481.9		-6509.9

[a]() indicate value is fixed in estimation.

values. With these initial estimates, the ML is employed. Results of the Standard model estimation are presented in Table IV.

For the SSFR3 model estimation, in addition to R_a and L_ℓ, L_{aq} is fixed to the value estimated for the Standard model. The damper windings are initialized as before. Results of the estimation are presented in Table IV. Note that the q-axis Standard and SSFR2 models are identical.

It is found that the SSFR3 model has a lower AIC value than the Standard model. However, it is not known if a model of higher order than the SSFR3 model is suitable. Therefore, the SSFR4 model, which has four rotor body circuits, is tested. It is found that this model is not physically realizable and has values of AIC and $V(\theta)$ that are higher than those of the SSFR3 model. The SSFR3 model is chosen as the most suitable equivalent circuit model.

XI. Q-Axis Model Standstill Validation

The estimated q-axis models are verified by comparing their simulated q-axis stator current responses against the measured standstill $i_q(t)$ response. For the q-axis transfer function and circuit models discussed above, it is again observed that the estimated model responses match the measured responses well. Fig. 4 shows the responses for the fourth order transfer function model.

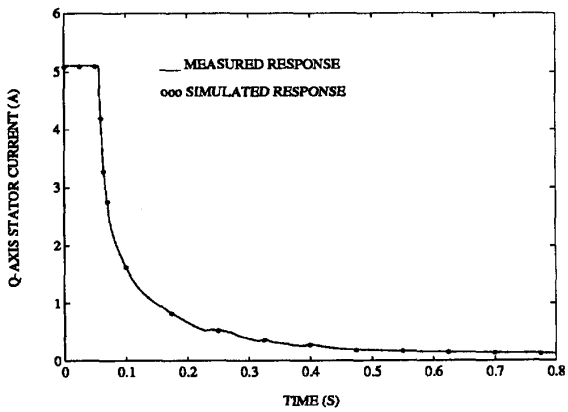

Fig. 4: Measured $i_q(t)$ response and simulated $i_q(t)$ response using the fourth order transfer function model.

XII. Small Disturbance Simulation Study

To observe the dynamic behavior of the standstill estimated models, simulation of a small disturbance test is performed for the 240 V, 5 kVA machine. In the experiment, the machine is tied to the system bus through a tap-changing transformer. Using the tap, the voltage at the machine terminals is adjusted to approximately 170 V or 70% of its rating. The machine is therefore underexcited, and no significant saturation effects are present. The disturbance is achieved by changing the excitation reference voltage by 2% to 5% of the steady state value. The machine runs at minimal load.

The simulation is performed using the d-q axis Standard model with parameter values as listed in Tables II and IV. The inputs are the measured terminal voltage, in terms of V_d and V_q, and the field voltage. The simulated outputs are the armature current, in terms of i_d and i_q, and the field current on the rotor side, i^*_{fd}. The speed is assumed constant at rated value.

The simulation is performed, and it is observed that the simulated outputs generally follow the transient characteristics of the machine. Therefore, the model exhibits good dynamic behavior. However, a steady state error exists between the simulated and measured currents: approximately 7% for $i_d(t)$, 6% for $i_q(t)$, and 18% for i^*_{fd}(t). For comparison purposes, Figs. 5, 6, and 7 show the measured and simulated responses without the steady-state error.

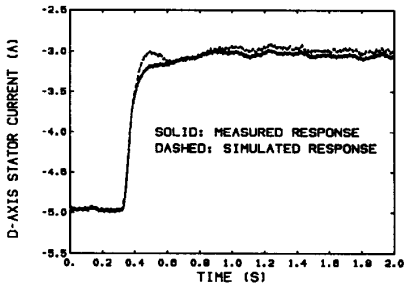

Figure 5: The measured and simulated $i_d(t)$ for the small disturbance test.

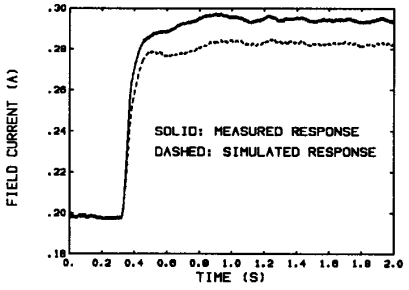

Figure 6: The measured and simulated field current on the rotor side, $i^*_{fd}(t)$, for the small disturbance test.

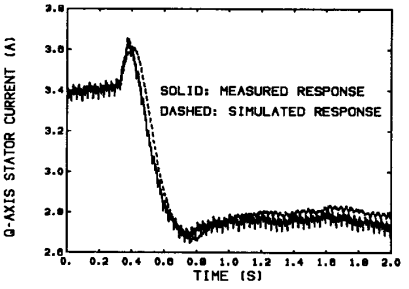

Figure 7: The measured and simulated $i_q(t)$ for the small disturbance test.

The results indicate that while the standstill time-domain data can be used to accurately model the machine at standstill, this data cannot provide sufficient dynamic information. The rotating machine exhibits hysteresis losses, friction and windage losses, rotational losses, and possible reduction in the end-ring contact impedance due to rotational forces. These phenomena are not represented by the standstill data and therefore cannot be reflected in the estimated parameters.

XIII. Conclusion

This paper presents a step-by-step procedure to identify the model order, the model structure, and the parameter values of the $d-q$ axis synchronous machine models using the standstill time-domain data. The flux decay test is performed on the 5 kVA salient pole synchronous machine. Physically realistic initial parameter values are computed based on the flux decay characteristics and the open/short circuit tests. The ML method is then able to converge to a unique set of parameters. Lastly, the Akaike Criterion is used to select the best-fit model structure.

This procedure yields standstill transfer function and equivalent circuit models which can accurately simulate the machine dc flux decay response. In addition, the small disturbance test results verify the basic validity of the standstill model structures identified. At the same time, the results indicate the need for on-line test data to complete the estimation process for the dynamic machine model.

Acknowledgment

The authors gratefully acknowledge the support of the National Science Foundation, Project ECS9015773.

References

[1] A. Keyhani, S. Hao, and R.P. Schulz, "Maximum likelihood estimation of generator stability constants using SSFR test data," *IEEE Transactions on Energy Conversion*, vol. 6, no. 1, pp. 140-154, March 1991.

[2] P.J. Turner, D.C. Macdonald, and A.B.J. Reece, "The D.C. decay test for determining synchronous machine parameters: measurement and simulation," *IEEE Transactions on Energy Conversion*, vol. 4, no. 4, pp. 616-623, Dec. 1989.

[3] P.J. Turner and D.C. Macdonald, "Transient electromagnetic analysis of the turbine generator flux decay test," *IEEE Transactions on Power Apparatus and Systems*, vol. PAS-101, no. 9, pp. 3193-3200, 1982.

[4] F.P. de Mello and J.R. Ribeiro, "Derivation of synchronous machine parameters from tests", *IEEE Transactions on Power Apparatus and Systems*, vol. PAS-96, no. 4, pp. 1211-1218, July/Aug. 1977.

[5] J.J. Sanchez-Gasca, C.J. Bridenbaugh, C.E.J. Bowler, and J.S. Edmonds, "Trajectory sensitivity based identification of synchronous generator and excitation system parameters," *IEEE Transactions on Power Systems*, vol. 3, no. 4, pp. 1814-1822, Nov. 1988.

[6] E.S. Boje, J.C. Balda, R.G. Harley, and R.C. Beck, "Time-domain identification of synchronous machine parameters from simple standstill tests," *IEEE Transactions on Energy Conversion*, vol. 5, no. 1, pp. 164-170, March 1990.

[7] P.L. Dandeno and A.T. Poray, "Development of detailed turbogenerator equivalent circuits from standstill frequency response measurements," *IEEE Transactions on Power Apparatus and Systems*, vol. PAS-100, no. 4, pp. 1646-1655, April 1981.

[8] "IEEE standard procedure for obtaining synchronous machine parameters by standstill frequency response testing," IEEE Std. 115A-1987.

[9] L.X. Le and W.J. Wilson, "Synchronous machine parameter identification: a time domain approach," *IEEE Transactions on Energy Conversion*, vol. 3, no. 2, pp. 241-248, June 1988.

[10] A. Keyhani and S.M. Miri, "Observers for tracking of synchronous machine parameters and detection of incipient faults," *IEEE Transactions on Energy Conversion*, vol. EC-1, no. 2, pp. 184-190, June 1986.

[11] K.J. Åström, "Maximum likelihood and prediction error methods," *Automatica*, vol. 16, pp. 551-574, 1980.

[12] H. Akaike, "A new look at the statistical model identification", *IEEE Transactions on Automatic Control*, vol. AC-19, no. 6, pp. 716-723, Dec. 1974.

[13] A.E. Fitzgerald, C. Kingsley, Jr. and S.D. Umans, *Electric Machinery.* New York, NY: McGraw-Hill Book Company, 1983.

[14] "IEEE guide for synchronous generator modeling practices in stability analyses," IEEE Std. 1110-1991.

[15] P.C. Krause, *Analysis of Electric Machinery.* New York, NY: McGraw-Hill Book Company, 1987.